Small-rotation-angle measurement using an imaging method

Takamasa Suzuki, MEMBER SPIE
Hideki Nakamura
Osami Sasaki, MEMBER SPIE
Niigata University
Faculty of Engineering
8050 Ikarashi 2
Niigata 950-2181, Japan
E-mail: takamasa@eng.niigata-u.ac.jp

John E. Greivenkamp, FELLOW SPIE
University of Arizona
Optical Sciences Center
Tucson, Arizona 85721
E-mail: greiven@arizona.edu

Abstract. A system of small-rotation-angle measurement based on fringe projection is proposed and demonstrated. This system has potential for a broad range of uses and robustness to external disturbances, because it requires no coherent light. The setup is very simple and applicable to automatic on-line measurement. Several measurements indicate a sensitivity of 3 arcsec. [DOI: 10.1117/1.1348385]

Subject terms: rotation-angle measurement; fringe projection; image processing; on-line measurement.

Paper 200091 received Mar. 8, 2000; revised manuscript received Aug. 25, 2000; accepted for publication Sep. 7, 2000.

1 Introduction

Measurement of a rotation angle[1] involves the use of such established measuring devices as interferometers[2] and autocollimators. While the former are extremely accurate, their use is usually limited, due to financial constrains and to the fact that they require an operating environment totally isolated from external disturbances. The latter, while being simple to use, take much longer to obtain the target measurement. Therefore, they are not suitable for automatic measurement.

The system we have proposed[3,4] is not based on either of the above methods, but on what is referred to as optical image processing or the fringe projection method.[5,6] We calculate the angle from the relative phase shift of the viewed grating image by means of the Fourier transform (FT) method.[7,8] Although the method bears some resemblance to Moiré deflectometry[9] it is unique in that it does away with the need for coherent light sources, expensive optical equipment, and Moiré fringes,[10–12] relying instead on a single grating.

The originality of our method lies in the direct detection of the relative phase shift between the viewed gratings imaged by noncoherent light. That produces many advantages in measurement. Its insensitivity to external disturbances ensures that is operationally robust. Image capturing and processing are managed by a computer, and the method requires little or no fine tuning, thus making it ideally suited to automatic on-line measurement. The detection range is also tunable by varying the spatial frequency of the grating or the distance between the test target and the CCD camera. Moreover, it is easy to introduce a technique of two-wavelength interferometry.[13,14] Therefore, the detection range is widely adjustable.

2 Principle

2.1 *Mathematical Formulas*

The principle of the small-rotation-angle measurement is shown in Fig. 1. It measures the angle between the reference mirror (M1) and the object mirror (M2), which rotates around the point of origin (O). A grating image projected simultaneously onto M1 and M2 is reflected to and observed on the viewing plane. The viewed grating images reflected by M1 and M2 are called the reference image and the object image, respectively, in this paper. If M2 slightly rotates by θ, the object image shifts by s with respect to the reference image. The shift s is represented by

$$s = d \tan 2\theta + x_0 \tan\theta \tan 2\theta, \tag{1}$$

and this is a function of viewing distance d, rotation angle θ, and x coordinate x_0 of the grating. Since x_0 is much smaller than d, and θ is very small, the second term of Eq. (1) can be neglected. Thus, the rotation angle θ can be calculated by

$$\theta = \frac{1}{2}\tan^{-1}\left(\frac{s}{d}\right). \tag{2}$$

We measure the phase difference $\Delta\alpha$ between the reference and the object image to calculate the shift s. The phases α_r and α_o of the reference and the object image are detected by means of the FT method. The value of $\Delta\alpha$ is given by

$$\Delta\alpha = \alpha_r - \alpha_o. \tag{3}$$

The shift s is then calculated by

$$s = \frac{p}{2\pi}\Delta\alpha, \tag{4}$$

where p is the grating pitch. The rotation angle θ is given by

$$\theta = \tfrac{1}{2}\tan^{-1}\phi, \tag{5}$$

 0091-3286/2001/$15.00

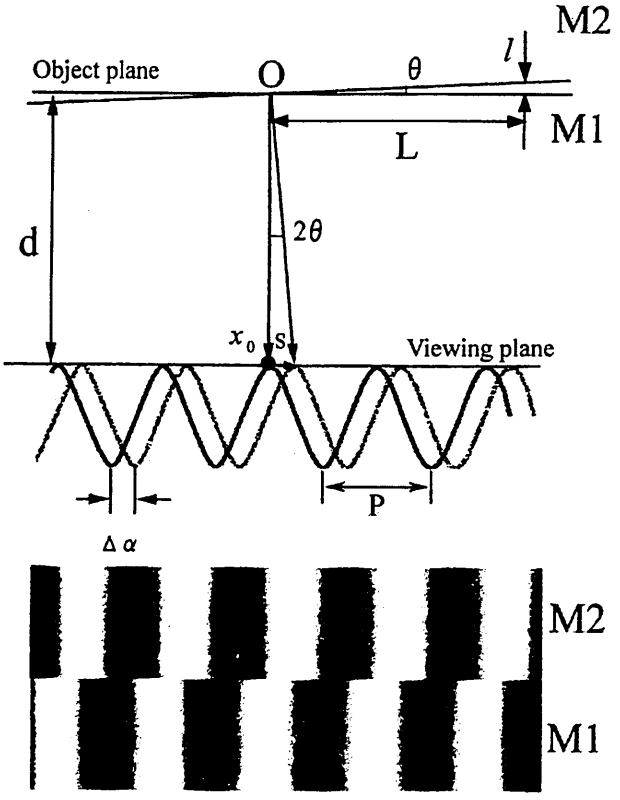

Fig. 1 Schematic of the rotation-angle measurement. M1, reference mirror;M2, object mirror; *s*, fringe shift; $\Delta\alpha$, phase difference; *P*, grating pitch; *d*, viewing distance.

where

$$\phi=\frac{p}{2\pi d}\Delta\alpha. \tag{6}$$

As $\Delta\alpha$ is wrapped in the region of $\pm\pi$, the maximum measurable range is given by

$$\theta_{\max}=\frac{1}{2}\tan^{-1}\frac{p}{d}. \tag{7}$$

Thus, the detection range can be adjusted by changing p and d.

When the phase difference $\Delta\alpha$ changes beyond $\pm\pi$ because of large rotation of the mirror, we cannot detect the actual $\Delta\alpha$. In this case, a technique of traditional two-wavelength interferometry[13,14] is useful. Suppose that we use two gratings that have different pitches p_1 and p_2. Since these different pitches are compared with different wavelengths, we call this method the two-grating method in this paper. Then the actual phase differences for each pitch are represented by

$$\Delta\tilde{\alpha}_1=\Delta\alpha_1+2m\pi=\frac{2\pi}{p_1}s \tag{8}$$

and

$$\Delta\tilde{\alpha}_2=\Delta\alpha_2+2n\pi=\frac{2\pi}{p_2}s, \tag{9}$$

where $\Delta\alpha_1$ and $\Delta\alpha_2$ are the detectable phase differences for p_1 and p_2, respectively, and m and n are integers. When the condition $m=n$ is satisfied, the difference $\Delta\alpha_s$ between $\Delta\tilde{\alpha}_1$ and $\Delta\tilde{\alpha}_2$ is calculated by

$$\Delta\alpha_s=\Delta\alpha_1-\Delta\alpha_2=\frac{2\pi}{p_s}s, \tag{10}$$

where

$$p_s=\frac{p_1p_2}{|p_1-p_2|} \tag{11}$$

is called the synthetic grating pitch. From Eqs. (8) and (10), the following holds:

$$p_s\Delta\alpha_s=p_1\Delta\tilde{\alpha}_1=p_1(\Delta\alpha_1+2m\pi). \tag{12}$$

The integer m is then derived as

$$m=\mathrm{INT}\left[\frac{R\Delta\alpha_s-\Delta\alpha_1}{2\pi}\right], \tag{13}$$

where $R=p_s/p_1$ is the ratio between the synthetic grating pitch and the original one, and the function INT[ ] gives the integer part of the argument. The actual phase difference $\Delta\tilde{\alpha}_1$ is obtained by substituting Eq. (13) into Eq. (8). If we use $\Delta\tilde{\alpha}_1$ instead of $\Delta\alpha$ in Eq. (6), a wide range of rotation-angle measurement can be achieved.

2.2 *Signal Processing*

The flow chart shown in Fig. 2 details the major steps in our process. After capturing the reflected image, some area to be processed is selected. The selected image is filtered to remove the nonuniformity of intensity and the high-frequency noise. A phase calculation is made by the FT method. In that method, the frequency components are calculated from the preprocessed image with the fast Fourier transform (FFT). After the frequency filtering, the inverse FFT is carried out to obtain the phase of the grating image. The FT method is applied both to the reference and to the object image. Then, the phase difference $\Delta\alpha$ is detected and the rotation angle θ is calculated by the formula described above.

2.3 *Calibration of the Viewing Distance*

In this system, we have to consider a systematic error depending on the viewing distance d and the grating period p. That error is given by

$$\Delta\phi=\frac{\partial\phi}{\partial p}\Delta p+\frac{\partial\phi}{\partial\delta}\Delta d=\frac{\Delta\alpha}{2\pi d}\left(\Delta p-\frac{p}{d}\Delta d\right). \tag{14}$$

This shows that we can reduce $\Delta\phi$ to zero by proper choice of the viewing distance d.

We assume that M2 is rotated by the micrometer head as shown in Fig. 1. The micrometer head is positioned at a

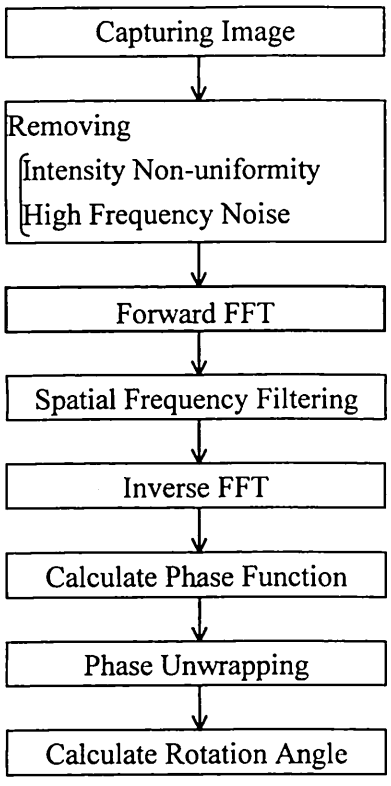

Fig. 2 Flow chart of the image processing.

distance L from the point of origin. First, we set the phase difference of viewed images to zero by rotating M2. Then, we push M2 by l until the phase difference becomes zero again. This means that the fringe shift s is equal to the grating pitch p. Therefore, we have the relationships

$$\tan\theta = \frac{l}{L} \tag{15}$$

and

$$\tan 2\theta = \frac{d}{p}. \tag{16}$$

Combining Eqs. (15) and (16), the correct viewing distance d is given by

$$d = \frac{L^2 - l^2}{2lL} p. \tag{17}$$

3 Experimental Setup

The experimental setup shown in Fig. 3 consists of a computer-generated grating, a CCD camera with an zoom lens, a computer, and a rotating-mirror system. A reference mirror M1, an object mirror M2, and a micrometer head from the rotating-mirror system. It is placed in front of the grating at a calibrated distance d of 280 mm. The inset in Fig. 3 shows how the object M2 is rotated around the point of origin O by means of a micrometer head, where "Forward" means pushout and "Reverse" means pullback of the mirror. The micrometer head is positioned at a distance

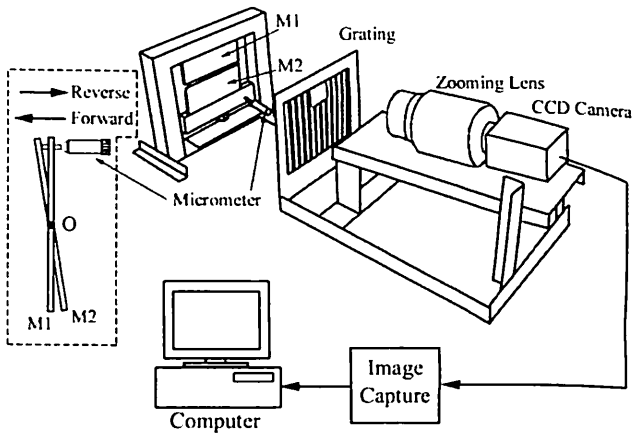

Fig. 3 Experimental setup: M1, reference mirror; M2, object mirror. Inset surrounded by dashed line shows how M2 is rotated.

L of 80 mm from the point of origin. The grating image reflected by the mirror is captured by the CCD camera through a small aperture that is in the upper middle of the grating. The pixel number and pixel pitch of the CCD camera are 768×494 and $6.4\,\mu\text{m}\times7.5\,\mu\text{m}$, respectively.

The captured images are then processed by a computer. No special lighting was employed during the conduct of this experiment. We relied, instead, upon ordinary room light. Since this system is a prototype, it uses two mirrors as a reference and an object in the experiments. Actually, however, this system requires only one object mirror if the object image is captured before it rotates.

We used two kinds of grating, a sinusoidal grating and a binary one, as shown in Fig. 4. They were printed with a laser-beam printer, which has resolution of 600 dots/in. The distortion of the grating was estimated by FFT analysis. The ratio in the power spectra between the fundamental component and the second harmonic was 5.8×10^{-3}. Moreover, as captured images are processed in the fre-

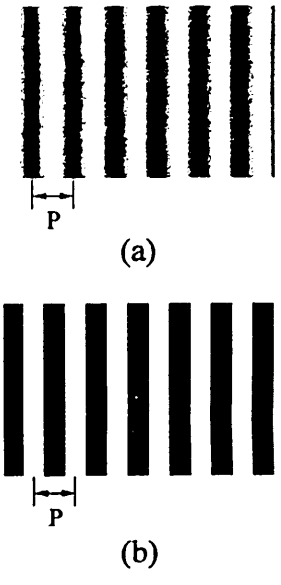

Fig. 4 Grating images used in the experiments.

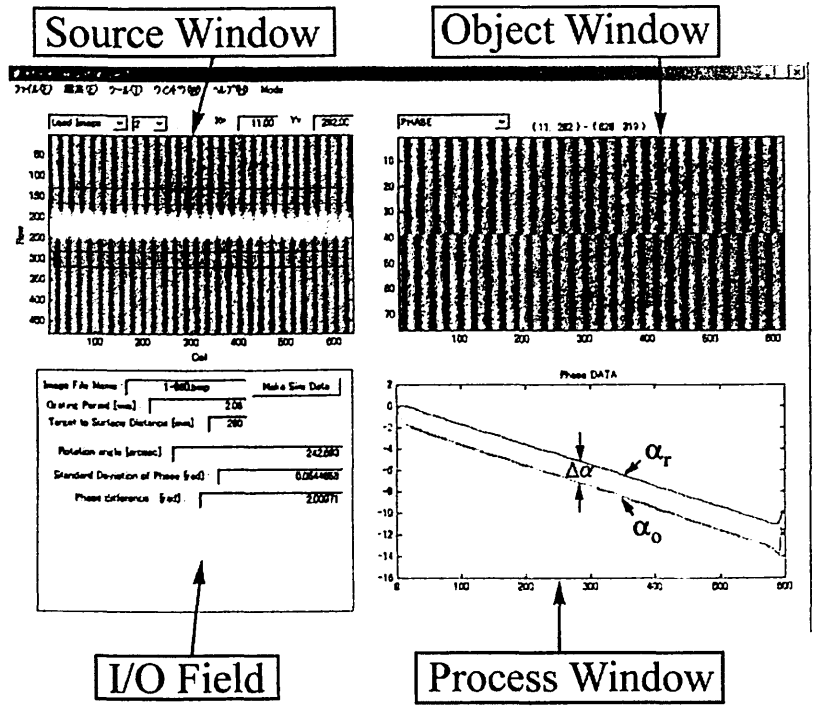

Fig. 5 Display of the image processing.

quency domain and only the fundamental component is used to calculate the phase, second-harmonic distortion is not very serious in our experiments.

4 Results

Figure 5 serves to explain the graphical user interface on the display of the computer. Results of the calculation for the captured image are displayed in this convenient window format. The original images reflected by M1 and M2 are displayed in the upper and lower areas of the source window, respectively. The images used in the phase analysis are cut from the source window and pasted in the object window. The phases α_r and α_o calculated from the reference and the object image, respectively, are displayed in the process window. Parameters such as grating pitch and viewing distance are displayed in the I/O field. Measurement results are displayed also in the I/O field.

First, we examined required cycle numbers of the grating for realizing a good measurement. Several calculations were made with a simulation. Measurement errors for different cycle numbers of the grating are shown in Fig. 6(a). It shows that good measurement accuracy can be achieved when we use more than six cycles. Moreover, Fig. 6(b), a magnification of Fig. 6(a), indicates that the measurement error is less than 0.1 arcsec if we use more than ten cycles of the grating in the signal processing (1 arcsec $=1/3600$ deg).

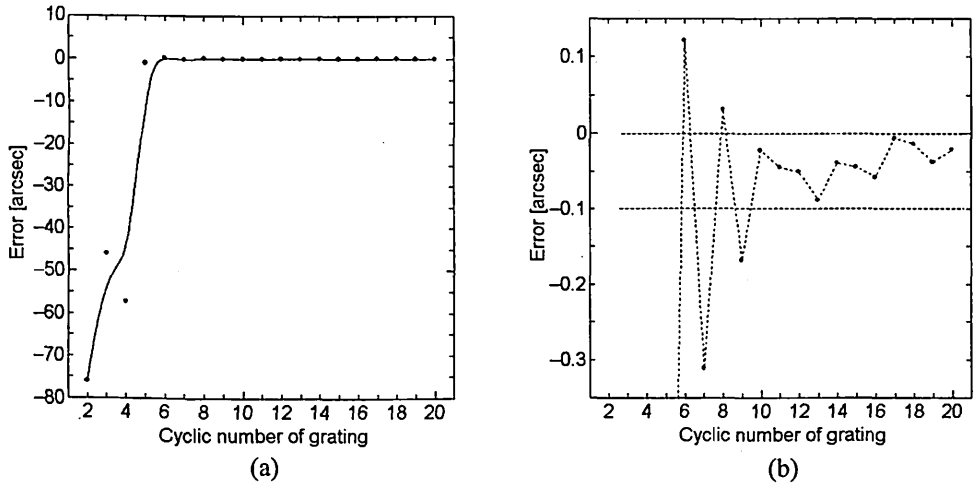

Fig. 6 Measurement error plotted against the cycle number of the grating: (a) overall plot and (b) magnification.

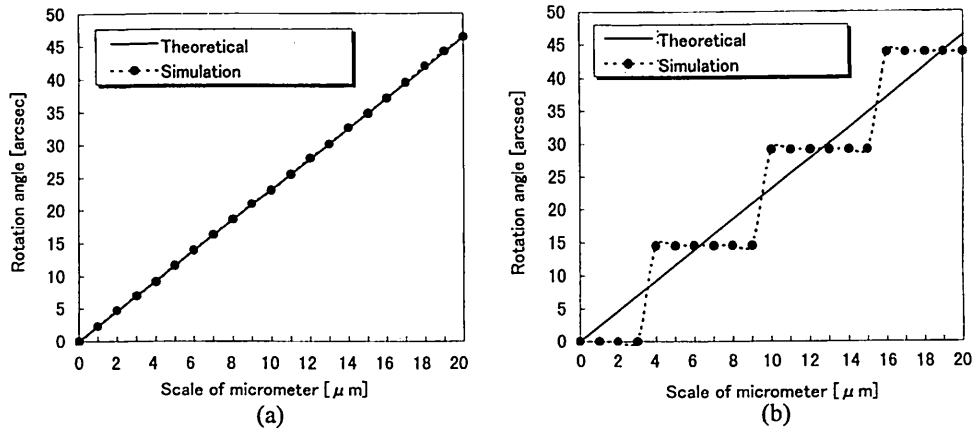

Fig. 7 Measurement error calculated by a simulation with (a) the sinusoidal grating and (b) the binary grating.

We made simulations to confirm the measurement accuracy. Figures 7(a) and 7(b) are the results obtained with the sinusoidal grating and the binary one, respectively. The grating pitch in both results was 2.06 mm. The x axis shows the displacement of M2 driven by the micrometer head. In these simulations, the travel pitch was 1 μm. The results detected by our method show good agreement with the theoretical curve for the sinusoidal grating as shown in Fig. 7(a). The measurement error was 0.105 arcsec rms. The result obtained with the binary grating has periodic measurement error as shown in Fig. 7(b). It is considered that the frequency resolution of the FT method was not so good for the binary grating.

We used the micrometer head to rotate M2 around the point of origin, noting each 1-μm shift, whether forward or backward. The conditions are same as the simulation shown in Fig. 7. Major results measured with the sinusoidal grating and the binary one are shown in Fig. 8. The grating pitch in both instances was 2.06 mm. The range of variation of the rotation angle was 50 arcsec in these experiments. Measurement errors both in forward and in reverse direction were less than 2 and 3 arcsec in rms, respectively, with respect to the sinusoidal grating and the binary one. The periodic error observed in the simulation disappeared in the experiment, as shown in Fig. 8(b), because the optical system forms a kind of low-pass filter and changes the binary grating to a quasisinusoidal one.

Results obtained when the object mirror M2 was driven with the travel pitch of 10 μm are shown in Fig. 9. The varied range of the rotation angle was 500 arcsec. When the sinusoidal grating was used, the measurement error was also less than 2 arcsec in both the forward and the reverse direction, as shown in Fig. 9(a). When the binary grating was used, measurement error was around 3 arcsec rms. We consider that these errors come from not only our measurement system but also the mirror-rotating system.

Next, we tried applying the two-grating method to expand the measurement range. The result obtained by the computer simulation is shown in Fig. 10(a). We used sinusoidal gratings whose pitches were 2.06 and 1.54 mm, respectively. The synthetic grating pitch p_s becomes 6.10 mm with these two gratings. It results in a measurement range of 1123 arcsec. Results measured with a single grating are shown by a dot-dash line and a dotted line, respectively. They are discontinuous because the phase differences $\Delta\alpha_1$ and $\Delta\alpha_2$ are wrapped in the region of $\pm\pi$. When the two-grating method was applied, however, the

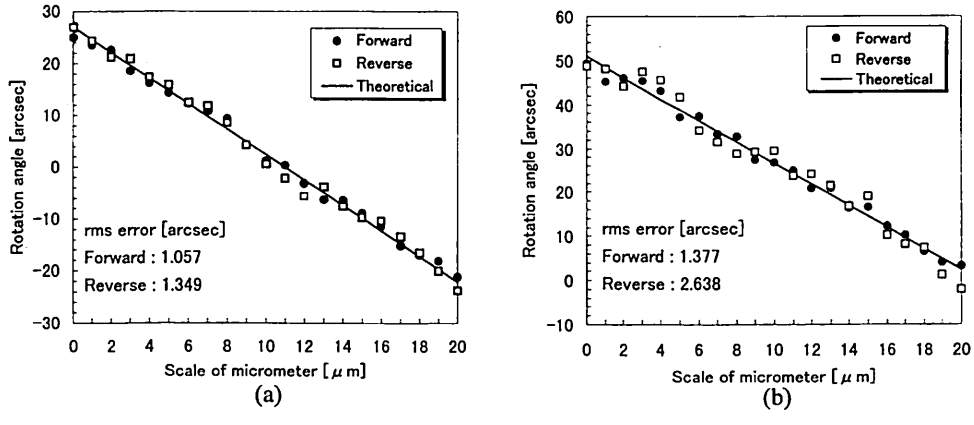

Fig. 8 Rotation angles measured with (a) the sinusoidal grating and (b) the binary grating. Travel pitches of the micrometer head are 1 μm.

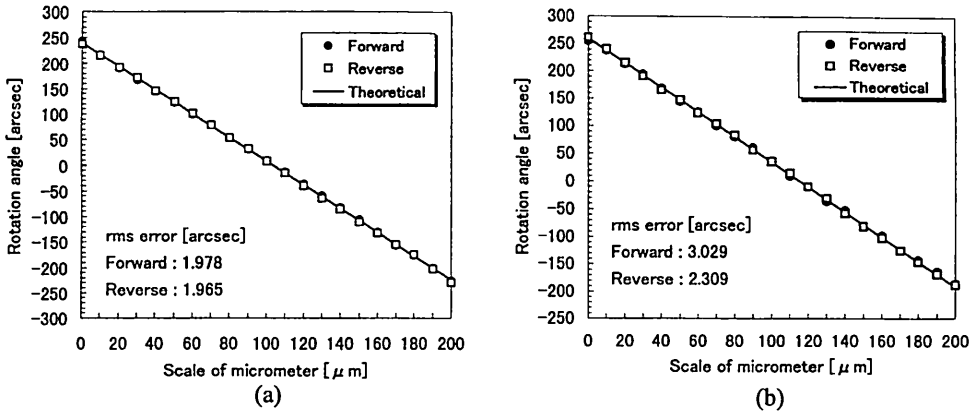

Fig. 9 Rotation angles measured with (a) the sinusoidal grating and (b) the binary grating. Travel pitches of the micrometer head are 10 μm.

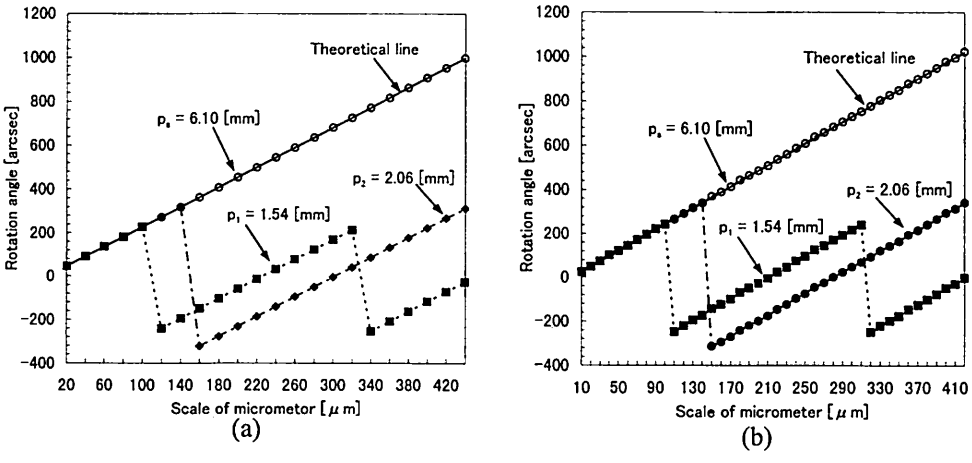

Fig. 10 Rotation angles measured in (a) the simulation and (b) the experiment. Plots on the dot-dash line and the dotted line are obtained by an ordinary method that uses a single grating. Plots on the solid line are obtained by a two-grating method.

rotation angle was detected without such discontinuities over the whole range. The results agree with the theoretical (solid) line. The measurement error was 0.114 arcsec rms.

The experimental result obtained by the two-grating method is shown in Fig. 10(b). The measurement conditions were same as those of the simulation. The results have a strong resemblance to those shown in Fig. 10(a). The error between the results and the theoretical line was 2.933 arcsec rms in this experiment.

5 Conclusion

In conclusion, we have proposed and demonstrated an accurate and wide-range small-rotation-angle measurement system. Our system has many advantages. It is simple in that it uses a noncoherent light source, a computer-generated grating transparency, and a CCD camera. Since it does not require a coherent light source, it is insensitive to external disturbance and works with rough alignment. We have shown the principles of measurement, the calibration, and the use of a two-grating method that expands the measurement range. Some computer simulations verified the measurement accuracy.

In the experiments, we measured several rotation angles of an object mirror that was driven by a micrometer head. The measured angles agreed well with the theoretical ones. They indicate a measurement accuracy of 3 arcsec. We think that a precise mirror-rotating system will be required to estimate the actual measurement error in our system.

Acknowledgments

The authors are grateful to Mr. H. Iwano for his help in the experiments. A part of this work was presented at an SPIE meeting.[3,4]

References

1. J. Z. Malacara, "Angle, distance curvature, and focal length measurements," Chap. 18 in *Optical Shop Testing*, D. Malacara, Ed., pp. 718–720, Wiley, New York (1992).
2. P. Shi and E. Stijns, "New optical method for measuring small-angle rotations," *Appl. Opt.* **27**, 4342–4344 (1988).

3. T. Suzuki, H. Nakamura, J. E. Greivenkamp, and O. Sasaki, "Rotation angle measurement using an imaging method," *Proc. SPIE* **3740**, 136–139 (1999).
4. T. Suzuki, H. Nakamura, J. E. Greivenkamp, and O. Sasaki, "Small rotation angle measurement using an imaging method," *Proc. SPIE* **3835**, 14–21 (1999).
5. K. Leonhardt, U. Droste, and H. J. Tiziani, "Microshape and rough-surface analysis by fringe projection," *Appl. Opt.* **33**, 7477–7488 (1994).
6. R. Windecker, M. Fleischer, and H. J. Tiziani, "Three dimensional topometry with stereo microscopes," *Opt. Eng.* **36**, 3372–3377 (1997).
7. M. Takeda, H. Ina, and S. Kobayashi, "Fourier-transform method of fringe pattern analysis for computer-based topography and interferometry," *J. Opt. Soc. Am.* **72**, 156–160 (1982).
8. M. Takeda and K. Mutoh, "Fourier transform profilometry for the automatic measurement of 3-D object shapes," *Appl. Opt.* **22**, 3977–3982 (1983).
9. O. Kafri and J. Glatt, "Moiré deflectometry: a ray deflection approach to optical testing," *Opt. Eng.* **24**, 944–960 (1985).
10. B. P. Singh, K. Varadan, and V. T. Chitnis, "Measurement of small angular displacement by a modified moiré technique," *Opt. Eng.* **31**(12), 2665–2667 (1992).
11. B. P. Singh, T. Goto, R. Sharma, A. K. Kanjilal, R. Narain, V. T. Chitnis, J. Liu, and Y. Uchida, "Tracking and dynamic control of the angular alignment position in a photolithographic mask aligner by the moiré interference technique," *Rev. Sci. Instrum.* **66**(3), 2658–2660 (1995).
12. J. Liu, H. Furuhashi, A. Torii, R. Sharma, V. T. Chitnis, B. P. Singh, J. Yamada, and Y. Uchida, "Automatic mask alignment in the θ direction using moiré sensors," *Nanotechnology* **6**, 135–138 (1995).
13. C. Polhemus, "Two-wavelength interferometry," *Appl. Opt.* **12**, 2071–2074 (1973).
14. K. Creath, "Step height measurement using two-wavelength phase-shifting interferometry," *Appl. Opt.* **26**, 2810–2816 (1987).

Takamasa Suzuki received his BE and ME degrees in electrical engineering from Niigata University in 1982 and from Tohoku University in 1984, respectively, and his PhD degree in electrical engineering from Tokyo Institute of Technology in 1994. He is an associate professor of electrical and electronic engineering at Niigata University. His research interests include optical metrology, optical information processing, and phase-conjugate optics.

Hideki Nakamura received his BE and MS degrees in electrical engineering from Niigata University in 1998 and 2000, respectively. His research interest involved optical metrology. He is currently working at Fujitsu Oasis Development Co., Ltd., Japan.

Osami Sasaki received his BE and ME degrees in electrical engineering from Niigata University in 1972 and 1974, respectively, and his PhD degree in electrical engineering from Tokyo Institute of Technology in 1981. He is a professor of electrical and electronic engineering at the Niigata University, and since 1974 he has worked in the field of optical measuring systems and optical information processing.

John E. Greivenkamp is a professor of optical sciences and ophthalmology at the University of Arizona. He is a fellow of SPIE and of the Optical Society of America. He currently serves on the SPIE Board of Directors and chairs the SPIE Publications Committee. He also serves on the OSA Board of Directors and is chair of the OSA Engineering Council. He served on the National Research Council Committee on Optical Science and Engineering (COSE). His research interests include interferometry and optical testing, optical fabrication, ophthalmic optics, optical measurement systems, optical systems design, and the optics of electronic imaging systems.